

Effects of Cations on the Structure, Dynamics and Vibrational Sum Frequency Generation Spectroscopy of Liquid-Vapor Interfaces of Aqueous Solutions of Monovalent and Divalent Metal Nitrates

Supplementary Information

Abhilash Chandra¹, Shinji Saito^{2,1,*} and Amalendu Chandra^{1,2,*}

¹ Department of Chemistry, Indian Institute of Technology Kanpur, Uttar Pradesh
208016, India

² Department of Theoretical and Computational Molecular Science, Institute of
Molecular Science, Myodaiji, Okazaki 444-8585, Japan

*Email: For correspondence, amalen@iitk.ac.in, shinji@ims.ac.jp

1 Structural Properties

1.1 Radial Distribution Functions

To investigate the distribution of nitrate ions around water molecules, we have calculated the SRDF for HW-ON and OW-ON atom pairs, where OW and HW denote the oxygen and hydrogen atoms of water, respectively, and ON represents the oxygen atom of nitrate ions. The SRDF is calculated for water molecules located at the interface and in the bulk, and the results are shown in Figures S6 and S7, respectively. For OW-ON atom pairs in interfacial water (Figure S6(a)), the first peak maximum appear at similar positions across all systems, which shows that the nitrate ions have a similar geometry. The position of the first maximum agrees with earlier studies.¹⁻³ In the case of bulk water (Figure S7(a)), the SRDF exhibits similar qualitative features, but the position of the first minimum is different. The position of the first minimum is influenced by the specific nature of the salts, with the NaNO_3 system exhibiting a larger distance. This behavior can be attributed to the more diffuse solvation shells in the NaNO_3 system. Also, the height of the first peak is lower for the NaNO_3 system compared to the $\text{Mg}(\text{NO}_3)_2$ and $\text{Ca}(\text{NO}_3)_2$ systems. The formation of contact ion pairs (CIPs) is more likely for monovalent cations than for divalent cations; as a result, the peak height of the OW-ON SRDF is reduced. In the SRDF of HW-ON atom pairs for interfacial water (Figure S6(b)), the first maximum and minimum, are located at similar positions across all systems. The first maximum at 1.85 Å arises from hydrogen-bonded pairs. The second peak is split into two sub-peaks, corresponding to non-hydrogen bonded pairs involving oxygen of nitrate and hydrogen of water. The positions of the first maximum and the split peaks agree well with earlier reported studies.¹ For bulk water (Figure S7(b)), the SRDF for HW-ON atom pairs shows peak positions consistent with those observed for interfacial water (Figure S6(b)).

We have also calculated the angular distribution of the angle formed by the HW-ON and OW-ON vectors, where HW and OW represent the hydrogen and oxygen atoms of water molecules, respectively, and ON denotes the oxygen atom of nitrate ions. The angular distribution was computed only for atom pairs where the HW-ON and OW-ON distances lie within the cutoff corresponding to the first solvation shell. We have shown the results in Figure S8. The distribution is relatively narrow and approaches zero for angles exceeding 24° , which shows that the hydrogen bond between water and nitrate ions is directional.

1.2 Average Electric Field

The empirical mapping of quantum mechanical quantities in this study is based on the projection of the electric field at the hydrogen atom along the O–H bond direction. Consequently, the intensity of the VSFG spectrum depends on the electric field on the H-atom along the O-H bond vector. In this section, we have calculated the average electric field for the O–H groups of water molecules located in different layers along the z -direction. To account for the orientation of the O–H bond vector, we have assigned a positive or negative sign to the electric field depending on whether the O–H bond was up-oriented or down-oriented, respectively.

In Figure S9, we have shown the depth dependence of the average electric field across all interfacial systems studied. In the topmost layer, the average electric field is negative for all interfacial systems due to the predominance of down-oriented hydrogen bonded

O–H groups over up-oriented dangling O–H groups. In contrast, in the layer immediately below the Gibbs dividing surface (GDS), the electric field is significantly positive for the $\text{Mg}(\text{NO}_3)_2$ and $\text{Ca}(\text{NO}_3)_2$ systems. Divalent cations produce a strong electric field due to their higher charge density, which changes the orientation of O–H groups of water molecules compared to neat water/vapor interface. Most O–H groups of water molecules become up-oriented (see Figure 7 of the Paper). Therefore, we get a significant and positive average electric field for $\text{Mg}(\text{NO}_3)_2$ and $\text{Ca}(\text{NO}_3)_2$ systems. Conversely, for the NaNO_3 system, the electric field produced by the monovalent cation (Na^+) is weaker; therefore, it has a less pronounced effect on the orientation of O–H groups compared to the $\text{Mg}(\text{NO}_3)_2$ and $\text{Ca}(\text{NO}_3)_2$ systems. Consequently, the average electric field in the layer below the GDS is less significant and negative for NaNO_3 system. The average electric field far from the GDS, towards the bulk, is approximately zero for all interfacial systems.

References

- [1] P. Banerjee and B. Bagchi, *J. Chem. Phys.*, 2018, **148**, 224504.
- [2] P. Banerjee, S. Yashonath and B. Bagchi, *J. Chem. Phys.*, 2016, **145**, 234502.
- [3] D. Schaefer, M. Kohns and H. Hasse, *J. Chem. Phys.*, 2023, **158**, 134508.

Table S1: Interfacial thickness δ_{10-90} and bulk density ρ_b , in g/cm^3 , of the mass density profiles for all interfacial systems studied here. Mass density is calculated by including contributions from both water and ions present in the systems.

Systems	ρ_b (gm/cm^{-3})	δ_{10-90} (\AA)
neat water/vapor	0.992	3.80
Mg(NO ₃) ₂	1.298	4.27
Ca(NO ₃) ₂	1.294	4.17
NaNO ₃	1.263	4.76

Table S2: Timescales (in ps) from the decay of second-rank orientational correlation function of CBW, ABW, and interfacial water molecules of the neat water/vapor interface system. τ_1 , τ_2 , and τ_3 are the three relaxation times of triexponential fits (Eq. 10 in the main text) with their respective weights a_1 , a_2 , and a_3 where $a_3=1-a_1-a_2$. The subscript in τ_3 column represents the uncertainty in last digit(s).

Regions	$\tau_1(a_1)$	$\tau_2(a_2)$	$\tau_3(a_3)$
Bulk	0.006(0.37)	0.26(0.13)	2.33 ₀ (0.50)
Interface	0.08(0.41)	0.27(0.20)	2.09 ₁ (0.39)

Table S3: Timescales (in ps) from the decay of second-rank orientational correlation function of CBW, ABW, and interfacial water molecules of the liquid/vapor interface of aqueous $\text{Ca}(\text{NO}_3)_2$ system. τ_1 , τ_2 , and τ_3 are the three relaxation times of triexponential fits (Eq. 10 in the main text) with their respective weights a_1 , a_2 , and a_3 where $a_3=1 - a_1 - a_2$. The subscript in τ_3 column represents the uncertainty in last digit(s).

Regions	$\tau_1(a_1)$	$\tau_2(a_2)$	$\tau_3(a_3)$
CBW	0.01 (0.17)	0.32 (0.18)	3.33 ₁ (0.65)
ABW	0.01 (0.22)	0.31 (0.23)	2.28 ₂ (0.55)
Interface	0.01 (0.44)	0.29 (0.22)	2.32 ₃ (0.34)

Table S4: Timescales (in ps) from the decay of second-rank orientational correlation function of CBW, ABW, and interfacial water molecules of the liquid/vapor interface of aqueous NaNO_3 system. τ_1 , τ_2 , and τ_3 are the three relaxation times of triexponential fits (Eq. 10 in the main text) with their respective weights a_1 , a_2 , and a_3 where $a_3=1-a_1-a_2$. The subscript in τ_3 column represents the uncertainty in last digit(s).

Regions	$\tau_1(a_1)$	$\tau_2(a_2)$	$\tau_3(a_3)$
CBW	0.01 (0.17)	0.28 (0.20)	2.18 ₂ (0.63)
ABW	0.01 (0.18)	0.29 (0.22)	1.98 ₁ (0.60)
Interface	0.01 (0.23)	0.29 (0.27)	2.12 ₂ (0.50)

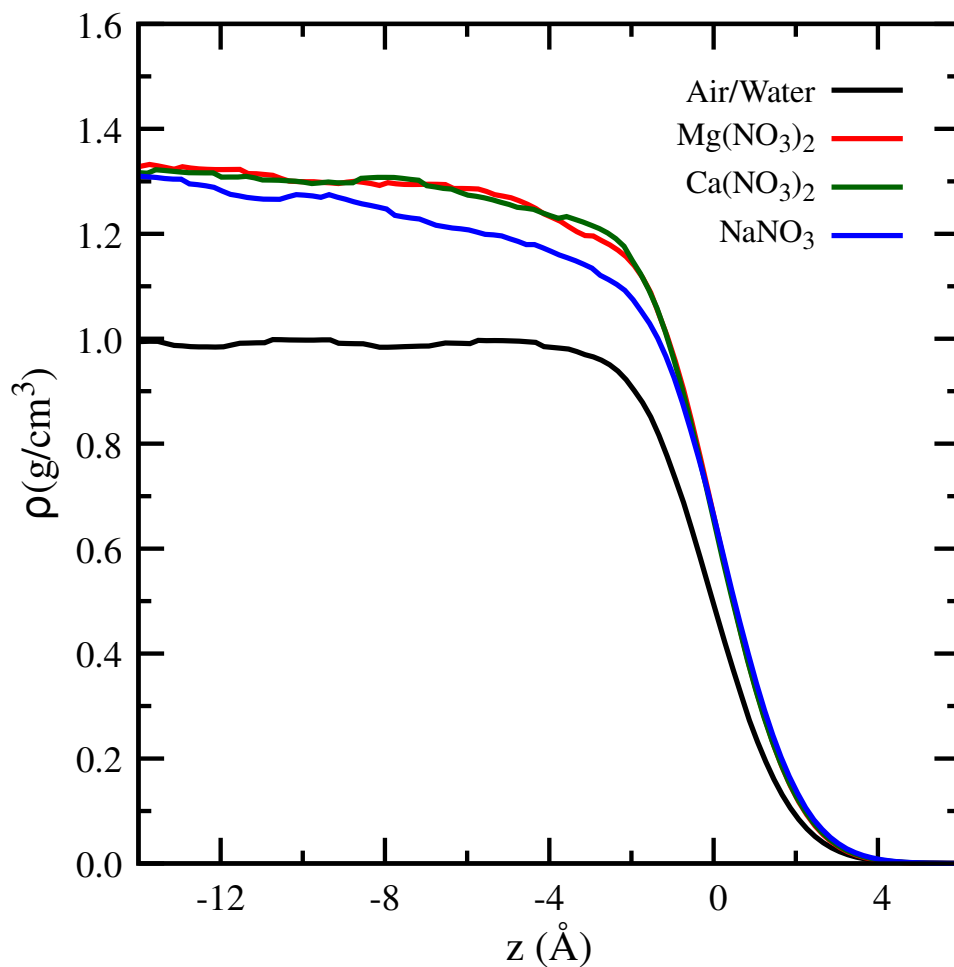


Figure S1: Mass density profile of liquid/vapor interface of aqueous $\text{Mg}(\text{NO}_3)_2$ (red), $\text{Ca}(\text{NO}_3)_2$ (green), and NaNO_3 (blue) solutions. Mass density calculated by including contributions from both water and ions present in the systems. Here $z = 0$ shows the location when the total mass density becomes half of the corresponding bulk density.

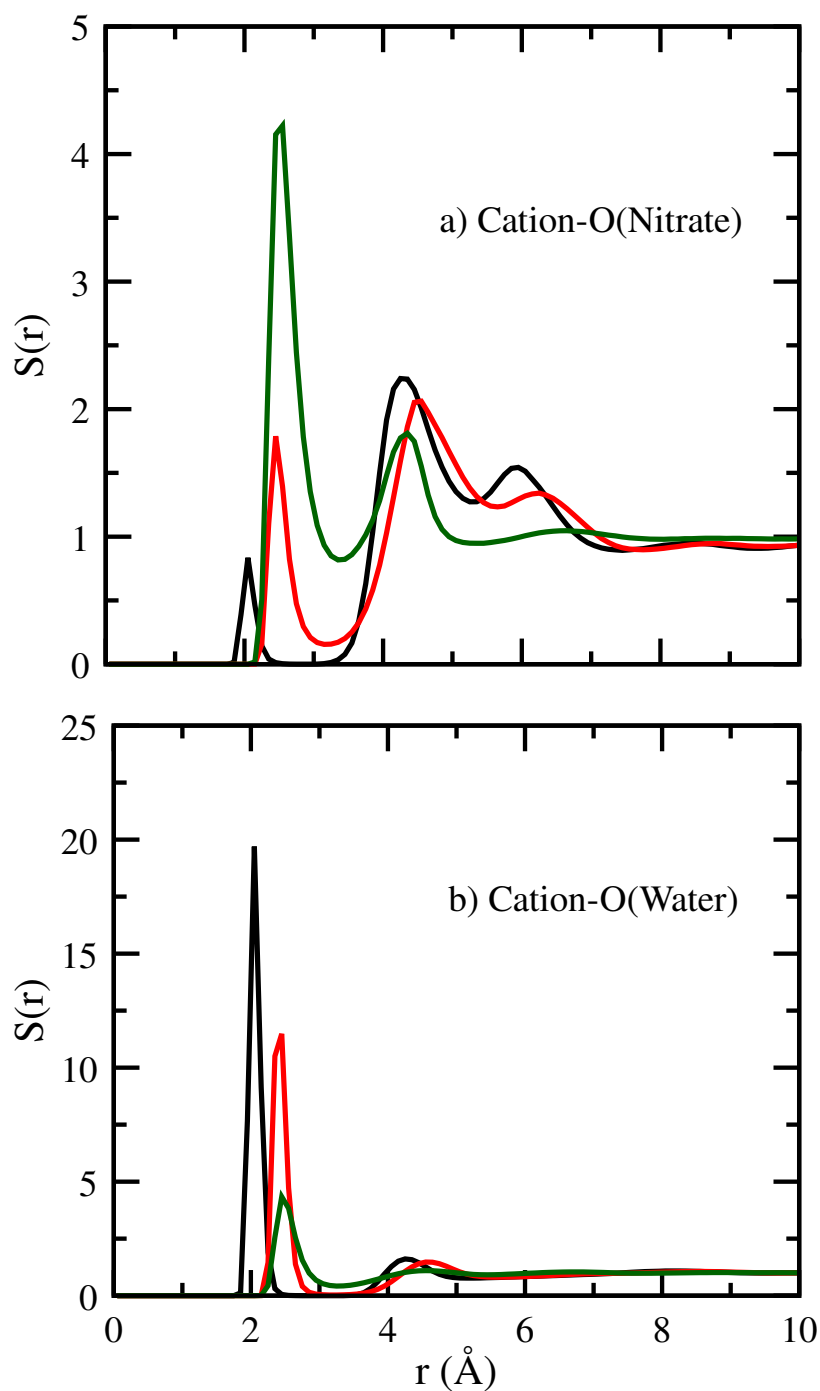


Figure S2: SRDF of (a) cation-oxygen (nitrates) and (b) cation-oxygen (water) pairs. The results of different systems of aqueous $\text{Mg}(\text{NO}_3)_2$, $\text{Ca}(\text{NO}_3)_2$, and NaNO_3 are represented by the black, red, and green curves, respectively. Here we have considered all water molecules (bulk and interface combined)

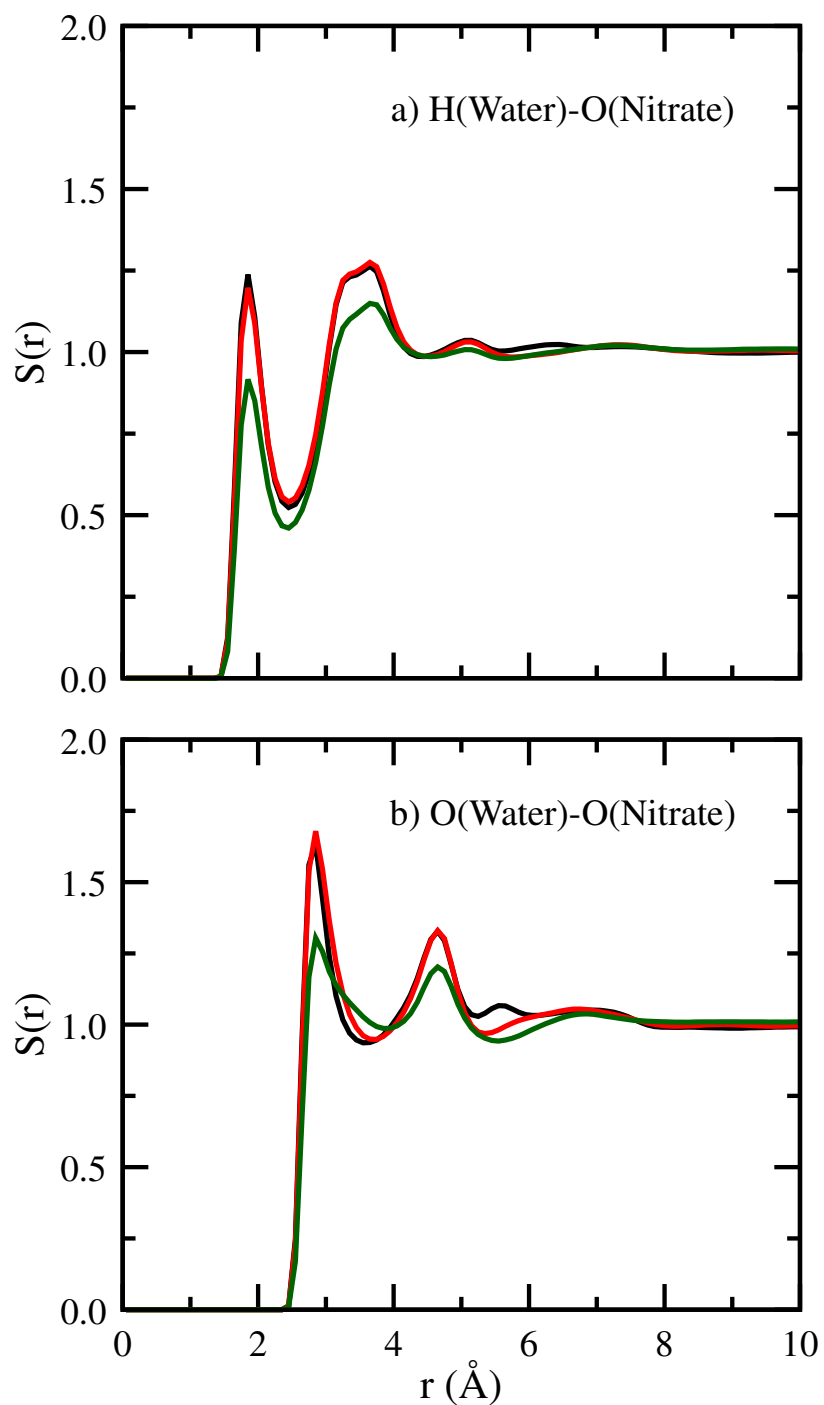


Figure S3: SRDF of (a) hydrogen (water)-oxygen (nitrates) and (b) hydrogen (water)-oxygen (water). The results of different systems of aqueous $\text{Mg}(\text{NO}_3)_2$, $\text{Ca}(\text{NO}_3)_2$, and NaNO_3 are represented by the black, red, and green curves, respectively. Here we have considered all water molecules (bulk and interface combined)

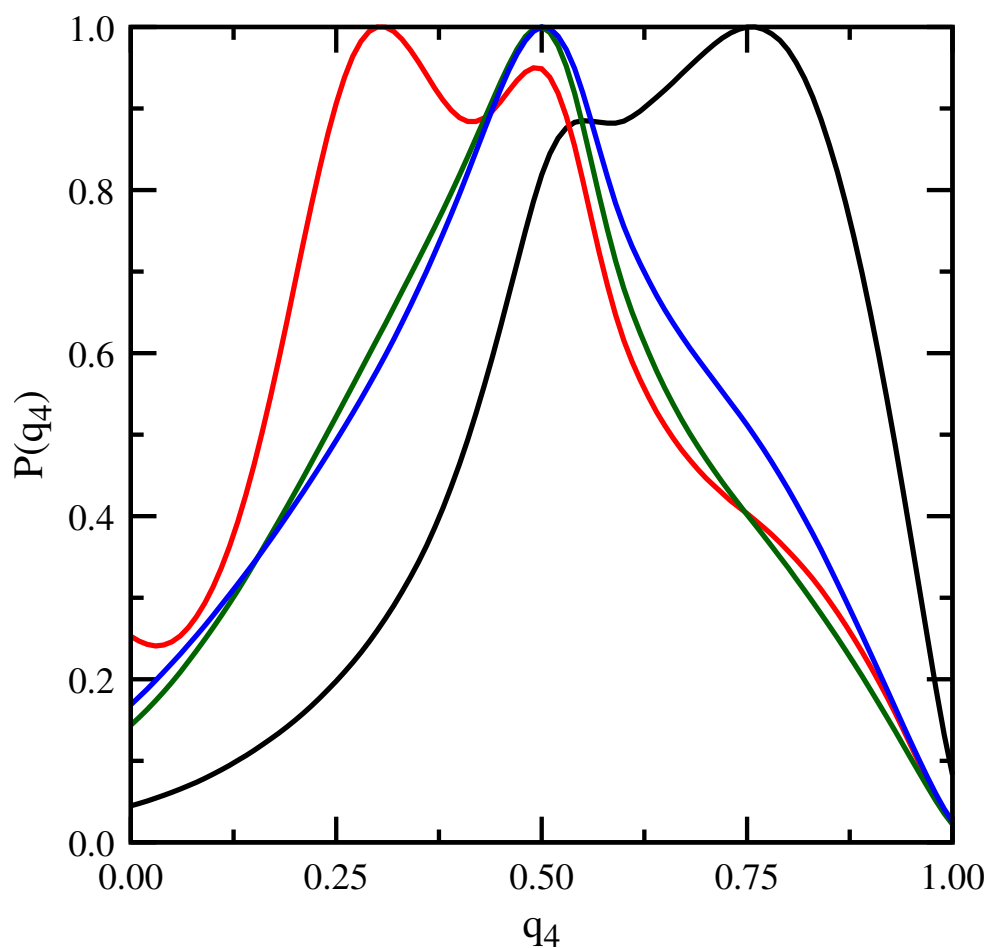


Figure S4: Tetrahedral order parameter of all water molecules (bulk and interface combined). The different systems of aqueous $\text{Mg}(\text{NO}_3)_2$, $\text{Ca}(\text{NO}_3)_2$, and NaNO_3 are represented by the black, red, and green curves, respectively. Here black curve represents neat water/vapor interfacial system.

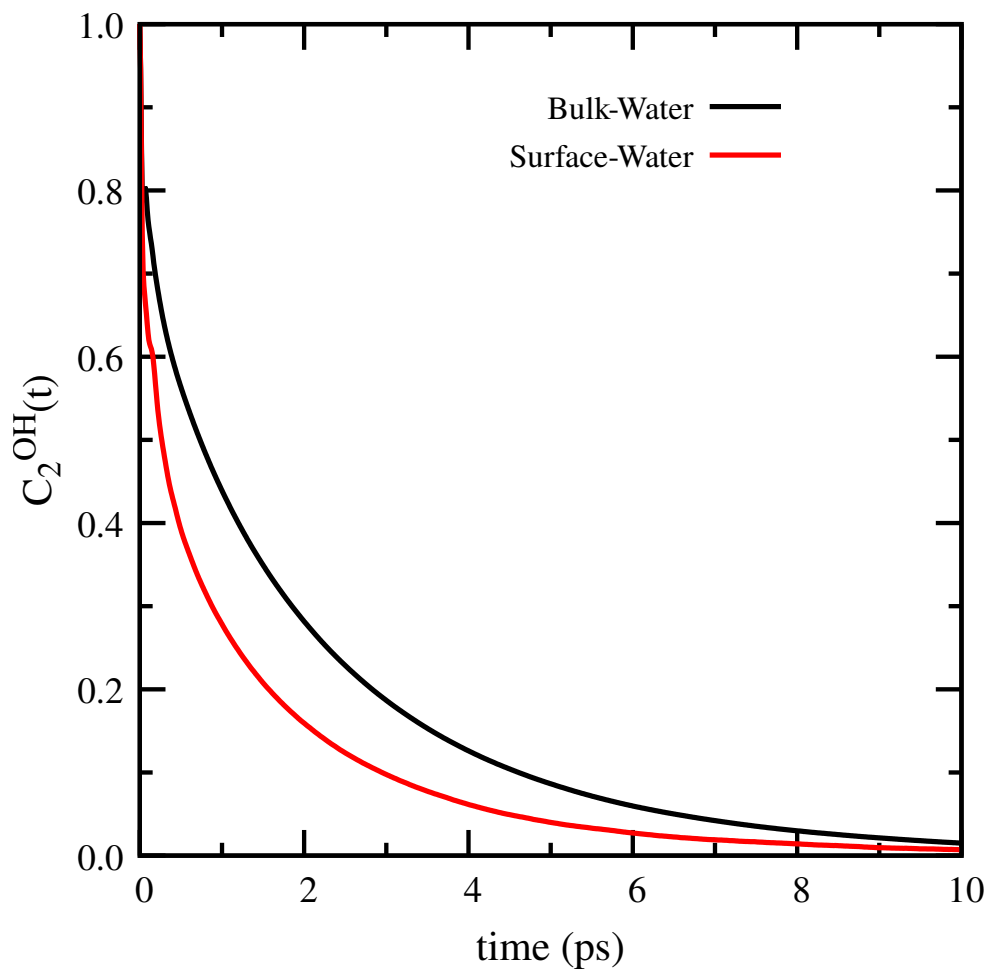


Figure S5: The decay of the second-rank orientational function, $C_2^{\text{OH}}(t)$, for the neat water/vapor interfacial system. The black curve represents the decay for water molecules in the bulk, while the red curve shows the decay for water molecules at the interface.

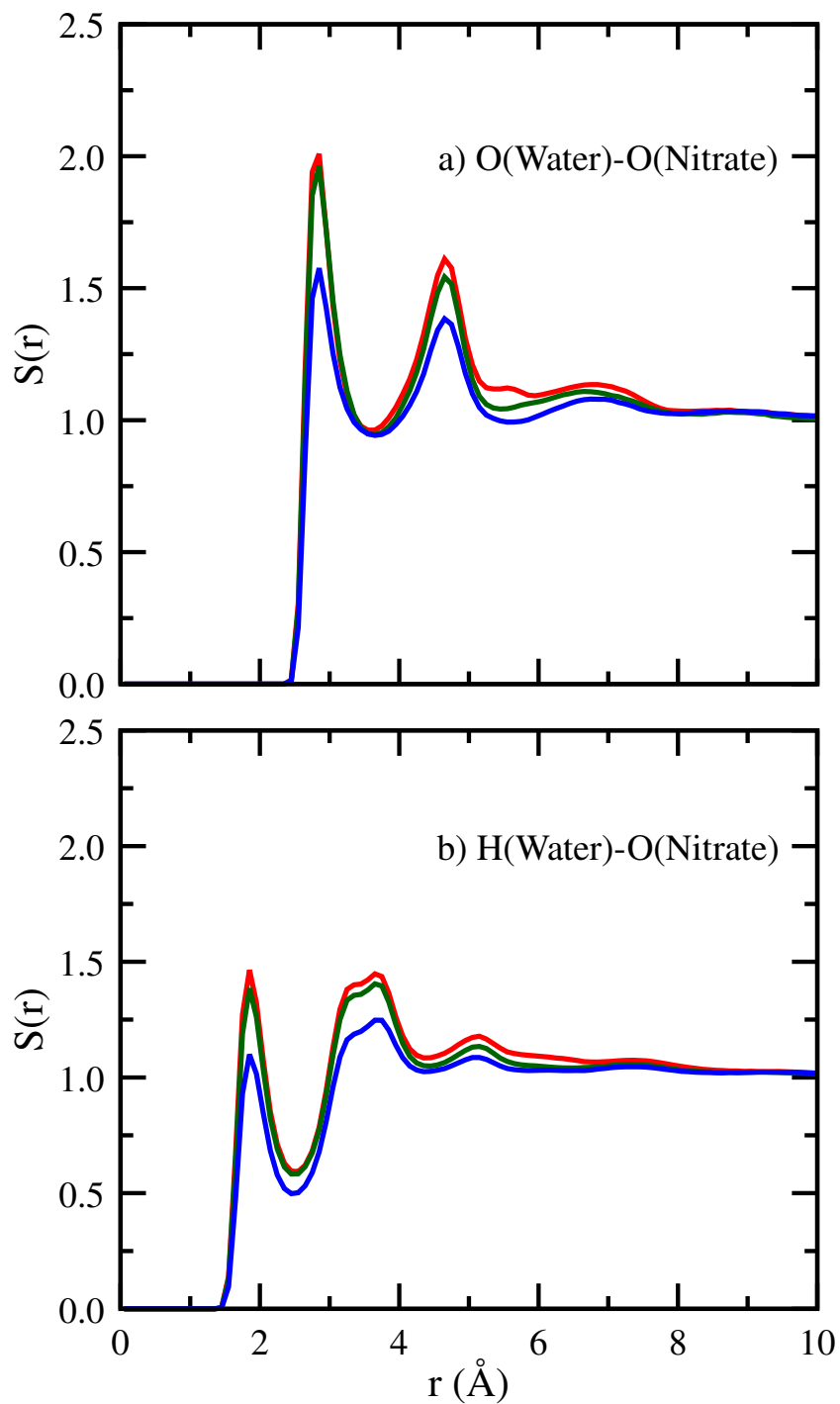


Figure S6: SRDFs for (a) O(water)-O(nitrate) and (b) H(water)-O(nitrate) pairs for water molecules at the interface. The results for aqueous Mg(NO₃)₂, Ca(NO₃)₂, and NaNO₃ systems are represented by red, green, and blue curves, respectively.

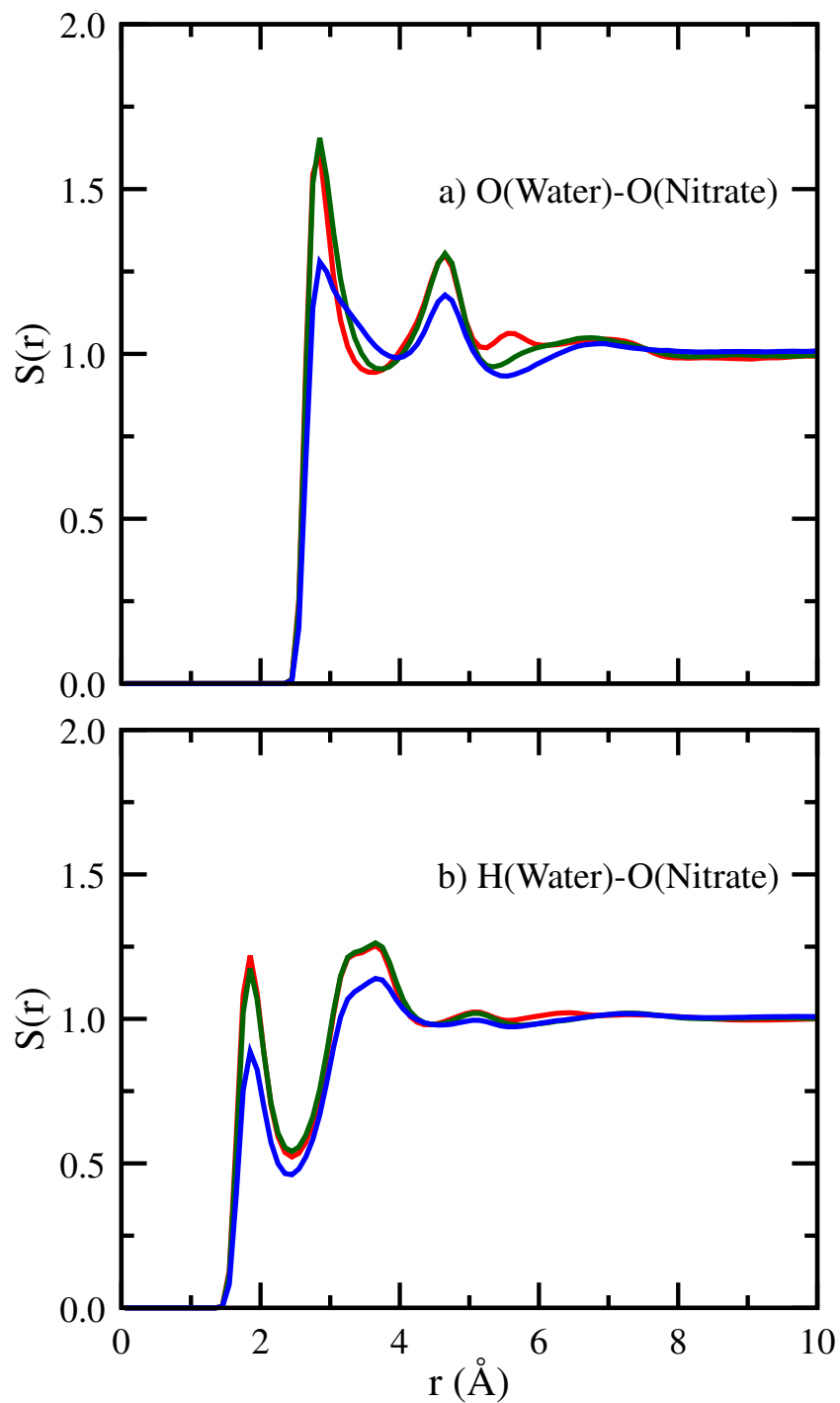


Figure S7: SRDFs for (a) O(water)-O(nitrate) and (b) H(water)-O(nitrate) pairs for water molecules in the bulk. The results for aqueous Mg(NO₃)₂, Ca(NO₃)₂, and NaNO₃ systems are represented by red, green, and blue curves, respectively.

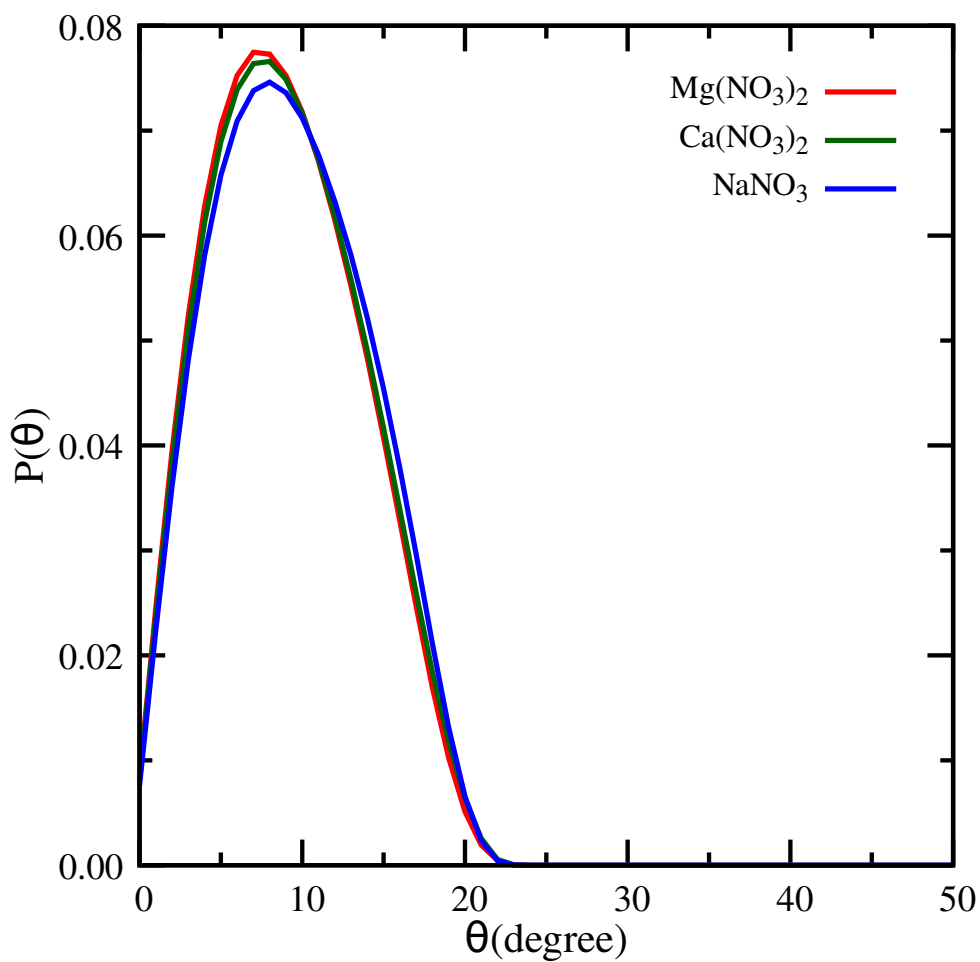


Figure S8: Angle distributions of the HW-ON and OW-ON vectors, where HW and OW represent the hydrogen and oxygen atoms of water, respectively, and ON denotes the oxygen atom of the nitrate ion. Angle distribution calculated for pairs where HW-ON and OW-ON distances lie within the first solvation shell cutoff of SRDF HW-ON and OW-ON, as shown in panels (a) and (b) of Figure S3.

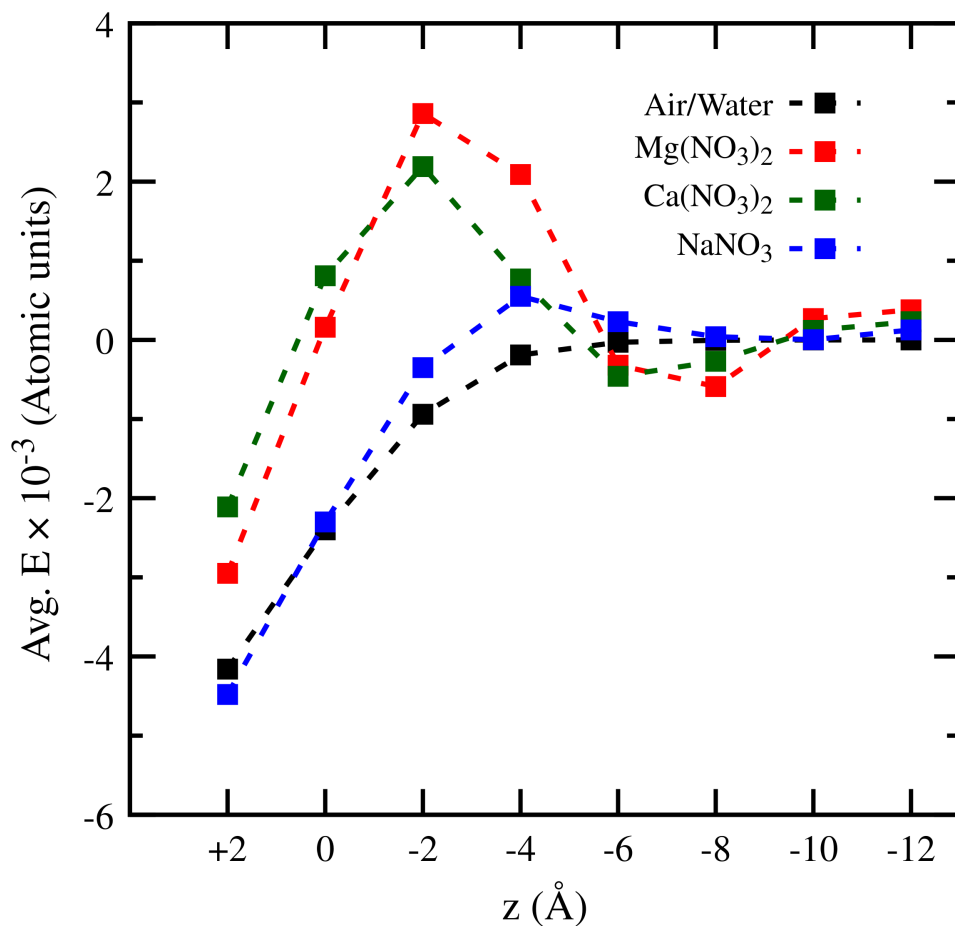


Figure S9: Average electric field calculated for the O-H groups of water molecules, layer by layer along the z -direction. The orientation of the O-H vector is also considered in this calculation: the electric field for an O-H group is taken as positive if the vector is up-oriented and negative if it is down-oriented. The $z = 0$ value on the x -axis corresponds to GDS, with the positive direction pointing towards the vapor phase and the negative direction towards the bulk phase.

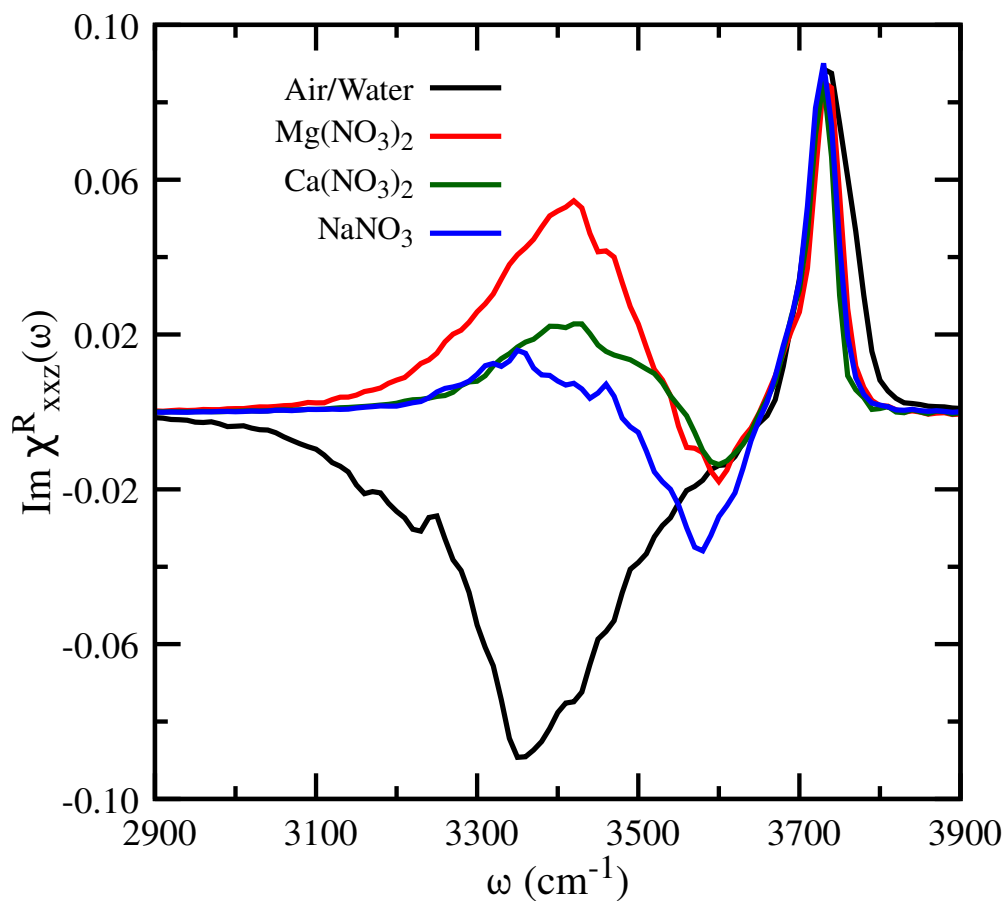


Figure S10: VSF spectra for aqueous $\text{Mg}(\text{NO}_3)_2$ (red curve), $\text{Ca}(\text{NO}_3)_2$ (green curve), and NaNO_3 (blue curve) solutions. The imaginary part of the VSF spectrum for the neat air/water interface is shown by the black curve for reference. VSF spectrum calculated for the final block of the trajectory. The simulation run was extended from 500 ps to 1 ns, and the spectrum was obtained for the first 800 ps of the extended trajectory.

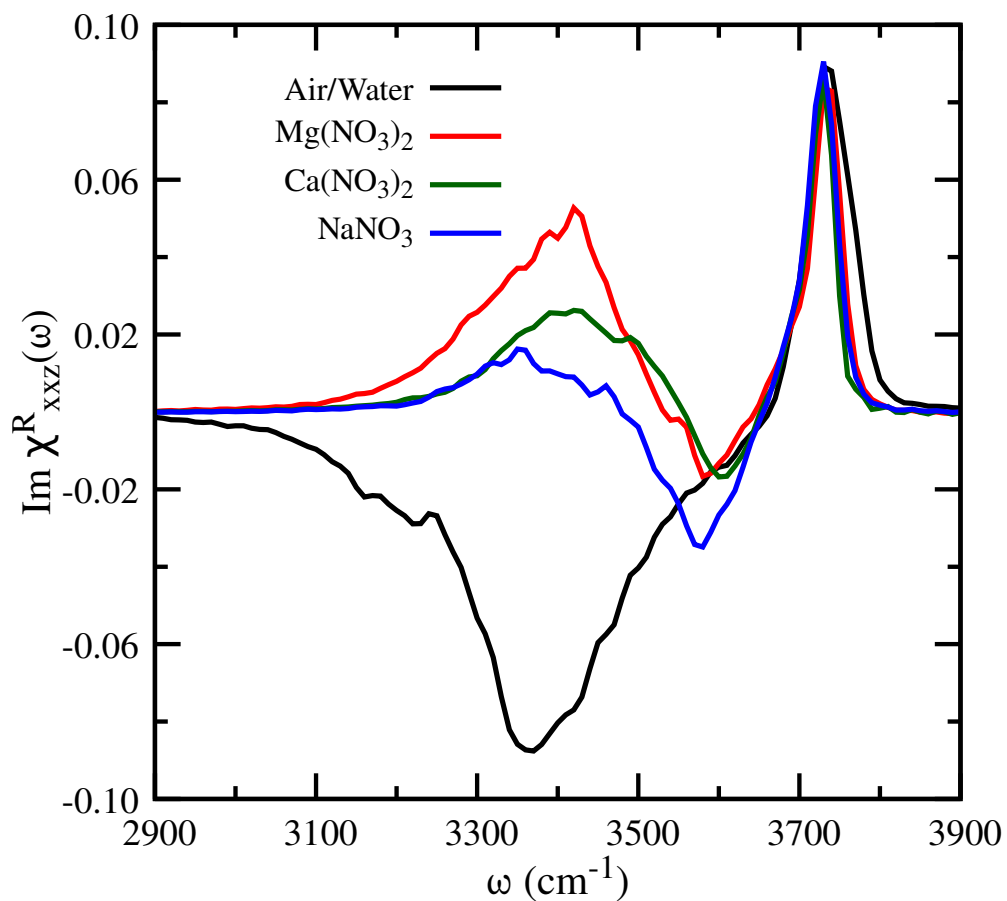


Figure S11: VSF spectra for aqueous $\text{Mg}(\text{NO}_3)_2$ (red curve), $\text{Ca}(\text{NO}_3)_2$ (green curve), and NaNO_3 (blue curve) solutions. The imaginary part of the VSF spectrum for the neat air/water interface is shown by the black curve for reference. VSF spectrum calculated for the final block of the trajectory. The simulation run was extended from 500 ps to 1 ns, and the spectrum was obtained for the total 1 ns of the extended trajectory.